A NON-LINEAR ANALYSIS FOR PLANE-STRAIN UNDRAINED PRESSUREMETER EXPANSION TESTS

Vincenzo Silvestri, École polytechnique de Montréal, Canada.
Badr Benabdellah, École polytechnique de Montréal, Canada.

ABSTRACT
This paper presents the solution for the undrained expansion of a cylindrical cavity in a non-linear workhardening soil. The solution is obtained using an inverse hyperbolic sine law to represent the relation between applied radial pressure and shear strain induced at the cavity wall. As in the case of a linearly elastic perfectly plastic (Tresca) material, three parameters are required to implement the solution, the initial horizontal pressure p_o, the undrained shear strength S_u, and the maximum shear modulus G_{max}. The values of these parameters are estimated in a particular case by linear regression analysis. Comparisons are also made with solutions obtained by means of power law, simple hyperbolic and linearly elastic perfectly plastic stress-strain relationships.

RÉSUMÉ
Cet article présente la solution pour l'expansion non-drainée d'une cavité cylindrique dans un sol non linéaire. La solution est obtenue en utilisant une loi sinus hyperbolique inverse décrivant la relation entre la pression radiale et la déformation de cisaillement. Comme dans le cas d'un matériau de type Tresca, trois paramètres sont nécessaires, la pression horizontale initiale p_0, la résistance au cisaillement non-drainé S_u, le module de cisaillement à l'origine G_{max}. Ces paramètres sont estimés dans un cas particulier à l'aide de régressions linéaires. Des comparaisons sont aussi effectuées avec des solutions obtenues en utilisant une loi de puissance, une relation hyperbolique simple, et un modèle Tresca.

1. INTRODUCTION

When the preconsolidation pressure σ'_p of soft natural clays, which is measured by means of constant strain rate (CRS) consolidation tests, is plotted as a function of the strain rate $\dot{\varepsilon}$ used, the resulting experimental relationship can be described by an inverse hyperbolic sine curve of the form (Silvestri et al. 1986):

$$\sigma'_p = \lambda + \mu \sinh^{-1}(\nu \dot{\varepsilon}) \qquad [1]$$

where λ is the value of σ'_p that would be measured in a CRS consolidation test performed at a strain rate $\dot{\varepsilon} = 0$, μ is a viscosity coefficient, and ν is a time coefficient. Such an equation is encountered when soil deformation is considered as a rate process (Mitchell 1993).

Curiously enough, when the applied total pressure p in a self-boring pressuremeter (SBP) test in clay is plotted as a function of the current shear strain γ inducted at the cavity wall, the resulting relationship is found to be quite similar to that given by Eq.1, except that the strain rate $\dot{\varepsilon}$ is replaced with the current shear strain γ, that is:

$$p = \lambda + \mu \sinh^{-1}(\nu \gamma) \qquad 0 \le \gamma \le 1 \qquad [2]$$

where, now, λ is the value of the pressure p (i.e., λ represents the horizontal geostatic stress p_o, when the borehole is not disturbed prior to the performance of the test), and μ and ν are material parameters.

It will be shown in the next section that the use of Eq.2 results in a non-linear workhardening stress-strain curve for clay.

2. STRESS-STRAIN RESPONSE

From the work of Hill (1950), Ladanyi (1972), and Palmer (1972) it is found that the stress-strain curve of clay may be obtained from the experimental measurement of radial pressure and shear strain, by using the following relationship:

$$\tau = \gamma \frac{dp}{d\gamma} \qquad [3]$$

where τ is the shear stress induced at the cavity wall, γ is the corresponding current shear strain ($0 \le \gamma \le 1$), and $dp/d\gamma$ is the slope of the radial pressure-shear strain curve.

Introducing Eq.3 into Eq.2 yields

$$\tau = \frac{\mu \nu \gamma}{(1 + \nu^2 \gamma^2)^{1/2}} \qquad 0 \le \gamma \le 1 \qquad [4]$$

Examination of this equation shows that when γ is very large (i.e., γ = 1), the shear stress is given by

$$\tau = \frac{\mu \nu \gamma}{(1 + \nu^2)^{1/2}} \qquad [5]$$

Since $\nu >> 1$ for most soft clays, as indicated below, then $\tau \approx \mu$ when $\gamma = 1$. Thus, the material parameter μ represents the undrained shear strength of the clay, S_u.

Differentiation of Eq.4 with respect to γ allows to determine the tangent shear modulus G:

$$\frac{d\tau}{d\gamma} = G = \frac{\mu\nu}{\left(1+\nu^2\gamma^2\right)^{3/2}} \quad [6]$$

Substituting $\gamma = 0$ into this equation permits to find the maximum shear modulus G_{max}:

$$\left.\frac{d\tau}{d\gamma}\right|_{\gamma=0} = G_{\max} = \mu\nu \quad [7]$$

The second material parameter ν is thus equal to:

$$\nu = \frac{G_{\max}}{\mu} = \frac{G_{\max}}{S_u} = I_r \quad [8]$$

where I_r is the rigidity index of the clay.

Because $\mu = S_u$ and $\nu = I_r$ from above, Eq.2 may also be written as:

$$p = p_0 + S_u \sinh^{-1}\left(I_r\gamma\right) \quad [9]$$

The limit pressure p_{limit} is found by putting $\gamma = 1$ in this equation leading to:

$$p = p_0 + S_u \sinh^{-1}\left(I_r\right) \quad [10]$$

In addition, as the rigidity index I_r, which is equal to ν, ranges between a minimum value of about 50 to a maximum value of 150 for soft clays, it follows that $I_r >> 1$. As a consequence, when a SBP test is pursued to strains of even as low as 10%, the inverse hyperbolic sine term in Eq.9 may be approximated by an exponential function of the form (Mitchell 1993):

$$\sinh^{-1}\left(I_r\gamma\right) \approx \ln\left(2I_r\gamma\right) \quad [11]$$

yielding

$$p = p_o + S_u \ln\left(2I_r\gamma\right) \quad [12]$$

which shows that the undrained shear strength can be obtained from the gradient (i.e., slope) of a plot of total applied pressure versus the natural logarithm of the current shear strain induced at the cavity wall.

Since $\mu = S_u$ and $\nu = I_r$ as before, the stress-strain curve of Eq.4 becomes:

$$\tau = \frac{G_{\max}\gamma}{\left[1+\left(I_r\gamma\right)^2\right]^{1/2}} \quad [13]$$

The curve described by this equation represents a non-linear workhardening constitutive relationship, as shown in Fig.1.

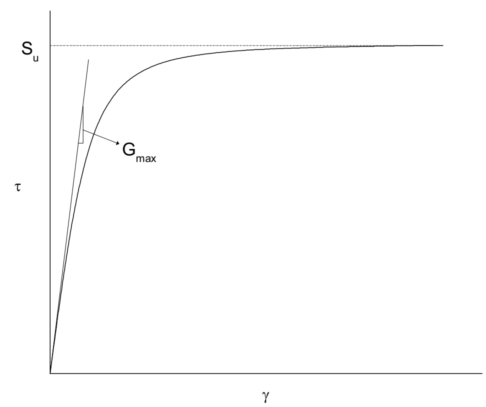

Figure1. Non-linear workhardening stress-strain curve.

3. APPLICATION

3.1 Inverse Hyperbolic Sine Low

The relationships given by Eqs.9 and 13 were applied to sel-boring (SBP) test data reported by Bolton and Whittle (1999). The results are compared with those obtained by these authors using a power law function. Further comparisons are carried out by assuming a simple hyperbolic stress-strain curve as well as a linearly elastic perfectly plastic response.

The experimental radial pressure versus shear strain curve is shown in Fig.2. The data was obtained by scanning and digitizing the original results of Bolton and Whittle (1999). In order to get the best fit to the data, the value of the undrained shear strength was first determined from the slope, at large strain, of the linear portion of the p-log γ relationship of Fig.2. This yielded S_u = 178 kPa, as also found by Bolton and Whittle (1999). Secondly, Eq.9 was transformed into:

$$\sinh\left(\frac{p-p_0}{S_u}\right) = I_r\gamma \quad [14]$$

Linear least-squares analyses were then carried out by assuming different values for p_0. Eq.14 was thus approximated by the straight line relationship:

$$\hat{y}_i = \hat{a}_i + \hat{b} x_i \qquad [15]$$

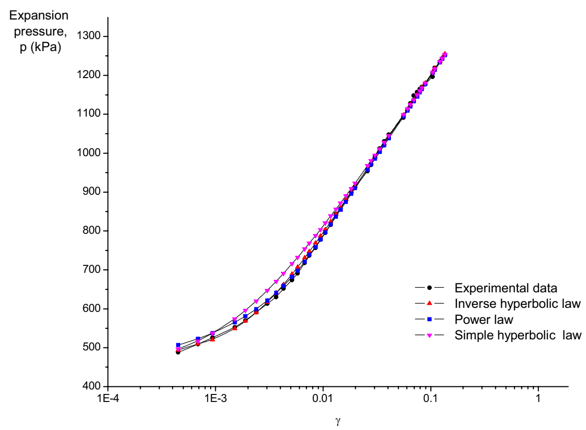

Figure2. Radial pressure-logarithm of current shear strain relationship.

where $\hat{y}_i$ is the estimated mean of sinh [(p - p_0) / S_u] for each x_i = γ_i, $\hat{a}_i$ is the intercept, and $\hat{b}_i$ is the slope (i.e., the estimated mean of I_r).

It was found that the values of the parameter p_0 reported in the first three rows of Table1 resulted in a very satisfactory fit to the data. Examination of the entries in this table indicates that the choice of p_0 = 460 kPa yields a slightly better fit, because it gives the highest value for the coefficient of correlation r (i.e., r = 0.99916). In this case, the estimated mean value of the rigidity index I_r equals 320.3.

However, as it would be expected that sinh [(p – p_0) / S_u] in Eq.14 should be zero when γ = 0, implying a straight line approximation passing through the origin (i.e., $\hat{a}_i$ = 0 in Eq.15), additional analyses were performed by forcing the regression line to pass through the origin. The results which are reported in the last four rows of Table 1 indicate that the choice of p_0 = 450 kPa yields, this time, a slightly better fit than the other values of p_0. The solutions given in Table 1 are, however, practically equivalent in that they all give a very good fit to the data, for the whole range of shear strains (i.e., $\gamma \leq 0.1353$). This notwithstanding, it was found that the initial part of the radial pressure versus shear strain relationship of Fig.2 (i.e., for $\gamma \leq 0.002$) was better approximated by using p_0 = 470 kPa with either $\hat{a}_i$ =0 and $\hat{b}_i$ = I_r =340.6 (r=0.99760) and $\hat{a}_i$ =0.0170 and = I_r $\hat{b}_i$ = 302.7 (r=0.99908). The curve shown in Fig.2 corresponds to Eq.9 with S_u = 178 kPa, p_0 = 470 Kpa, $\hat{a}_i$ = 0, $\hat{b}_i$ = Ir = 304.6. As these parameters imply G_{max} = S_uIr = 54219 kPa (54.2 MPa), the corresponding stress-strain curve is:

$$\tau(kPa) = \frac{54219\,\gamma}{\left[1 + (304.6\,\gamma)^2\right]^{1/2}} \qquad [16]$$

Examination of the curve described by this equation, which is shown in Fig.3, indicates that the shear stress τ reaches a horizontal asymptote for large strain. As for the values of the limit pressure p_{limit}, calculated on the basis of Eq.10, Table 1 shows that these are quite insensitive to the choice of the parameters $\hat{a}_i$ and $\hat{b}_i$. Indeed, the limit pressure varies from 1610.1 kPa to 1611.5 kPa.

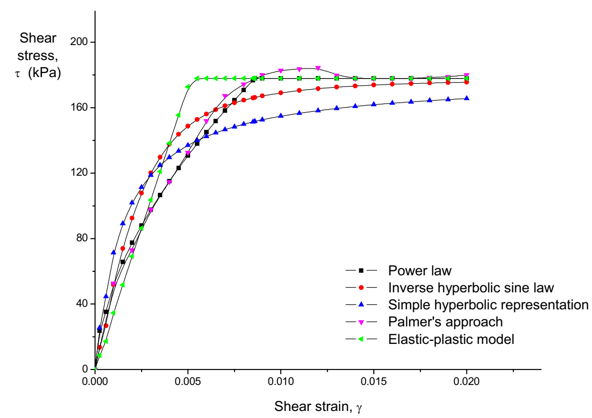

Figure3. Stress-strain curves.

3.2 Power Law Representation

The radial pressure versus shear strain relashionship of Fig.2 was approximated using the power law of Bolton and Whittle (1999). These authors proposed that the stress-strain curve be represented by:

$$\tau = \eta \beta \gamma^{\beta} \qquad \gamma \leq \gamma_y \qquad [17a]$$

and

$$\tau = S_u \qquad \gamma > \gamma_y \qquad [17b]$$

where η and β are material parameters, with $\beta < 1$ and $\gamma_y = (S_u/\eta\beta)^{1/\beta}$ is the shear strain at yield. It should be also noted that complete solutions for the expansion of both spherical and cylindrical cavities, based exactly on this same assumption, were published by Ladanyi and Johnson (1974), and Ladanyi (1975). The power law function in Eq.17 describes a non-linear elastic perfectly plastic (Tresca) model. The corresponding radial pressure versus shear strain curve is:

$$p = p_0 + \eta \gamma^{\beta} \qquad \gamma \leq \gamma_y \qquad [18a]$$

and

$$p = p_0 + S_u\left[\frac{1}{\beta} + \ln\left(\frac{\gamma}{\gamma_y}\right)\right] \qquad \gamma > \gamma_y \qquad [18b]$$

In addition, the limit pressure is found by putting $\gamma = 1$ into Eq.18b.

The values of the parameters β and η were determined by Bolton and Whittle (1999) using unload / reload loops. On the basis of the last two loops reported by these investigators, which resulted, respectively, in ln η_1 = 8.326 and β_1 = 0.5758, with r = 0.99955 and ln η_2 = 8.3505 and β_2 = 0.573, with r = 0.99960, the corresponding average values of ln η and β are: ln η = 8.3383 or η = 4181 kPa and β = 0.5744. As $\gamma_y = (S_u/\eta\beta)^{1/\beta}$ from Eq.17, the shear strain at yield is equal to 0.01078 for S_u = 178 kPa, η = 4181 kPa, and β = 0.5744. However, Bolton and Whittle (1999) retained β = 0.57 and γ_y = 0.0086, corresponding to η = 4698 kPa. In addition, these authors found that p_0 = 449 kPa, represented a satisfactory geostatic stress value. Eq.18 was, therefore, used with p_0 = 449 kPa, S_u = 178 kPa, γ_y = 0.0086, η = 4698, and β = 0.57 to plot the radial pressure versus shear strain relationship. This curve is also shown in Fig.2. Comparison between the numerical relationship based upon Eq.18 with that obtained using the inverse hyperbolic sine indicates that the two are quite similar.

The corresponding stress-strain curve, based upon Eq.17, is reported in Fig.3. Comparison between the curves shown in this figure indicates that the strain-stress relationship obtained by means of the inverse hyperbolic sine law is stiffer than the one based upon the power law, in the range $0.001 \le \gamma \le 0.007$.

Furthermore, in order to determine whether the material parameters β and η could be also obtained from the initial portion of the pressure-expansion curve (i.e., for $\gamma_y \le 0.01087$), without having to use the unload / reload loops, Eq.18 was first transformed into:

$$\ln(p_0 - p) = \ln\eta + \beta\ln\gamma \qquad [19]$$

and then approximated by the regression line of Eq.15, where $\hat{y}_i$ is now the estimated mean of ln (p-p_0) for each value of $x_i = \ln\gamma_i$, $\hat{a}_i = \ln\eta$ is the intercept, and $\beta = \hat{b}_i$ is the slope. Regression analyses were again performed by assuming different values for p_0. The results are reported in Table 2. In this table are also given the values of $\gamma_y = (S_u/\eta\beta)^{1/\beta}$. Examination of the various entries indicates that the choice of p_0 =420 kPa constitutes the best fit to the data with $\hat{a}_i$ = ln η = 8.3688 or η = 4308 kPa, $\hat{b}_i = \beta$ = 0.535, and r = 0.99969. Recalling that the results retained by Bolton and Whittle (1999) were η = 4698 kPa, β = 0.57, γ_y = 0.0086 with r = 0.9996, it appears that these correspond to a choice of p_0 close to 430 kPa in Table 2.

As for the values of the limit pressure p_{limit}, determined on the basis of Eq.18b for γ = 1, Table 2 indicated that these vary between 1602.6 kPa and 1610.1 kPa.

3.3 Simple Hyperbolic Representation

In order to determine whether a simple hyperbolic stress-strain curve of the form:

$$\tau = \frac{G_{\max}\gamma}{1 + I_r\gamma} \qquad [20]$$

could also be successfully used, this equation was substituted in Eq.2 to obtain the radial pressure versus shear strain curve. This resulted in:

$$p = p_0 + S_u \ln(1 + I_r\gamma) \qquad [21]$$

For γ very large, $I_r\gamma >> 1$, and Eq.21 may be approximated by:

$$p = p_0 + S_u \ln(I_r\gamma) \qquad [22]$$

indicating, once again, that the undrained shear strength can be obtained from the slope, at large strain, of a plot of total pressure versus the natural logarithm of the shear strain. In order to carry out linear regression analyses, Eq.21 was first transformed into:

$$e^{\left(\frac{p-p_0}{S_u}\right)} - 1 = I_r\gamma \qquad [23]$$

and then approximated by the regression line of Eq.15, where this time $\hat{y}_i$ is the estimated mean value of $[e^{(p-p0)/Su}-1]$ for each value of $x_i = \gamma_i$, $\hat{a}_i$ is the intercept, and $\hat{b}_i = I_r$ is the slope. Results of these regression analyses are summarized in Table 3 for different values of p_0. Although the calculated values of the coefficient of correlation r reported in this table are quite high, it was found that none of the regression equations could satisfactory approximate the radial pressure versus shear strain relationship for shear strain $\gamma \le 0.01316$. This is due to the presence of the negative $\hat{a}_i$ term. As a consequence, additional regression analyses were performed by forcing the regression line to pass through the origin (i.e., $\hat{a}_i$ = 0). The results are also reported in Table 3. Examination of the entries shown indicates that the choice of p_0 = 450 kPa constitutes the best fit to the data (r = 0.99793), yielding $\hat{b}_i = I_r$ = 669.5. These parameters (i.e., p_0 = 450 kPa, I_r = 669.5, S_u = 178 kPa and $G_{max} = I_r S_u$ = 119171 kPa) were then introduced into Eqs.20 and 21 to plot both the stress-strain curve and the radial pressure versus shear relationship, as shown in Figs.2 and 3. Examination of the predicted values of the total pressure p in Fig.2 indicates that they overestimate the actual trend at low moderate shear strain (i.e., for $\gamma \leq 0.03$). Concerning the hyperbolic stress-strain curve plotted in Fig.3, it appears that it is initially much stiffer than both the power law and inverse hyperbolic sine relationships.

As an additional point concerning the stress-strain curves reported in Fig.3, discrete data points, obtained from a direct application of Palmer's approach (i.e., Eq.2), were scaled from the results reported by Bolton and Whittle (1999) and are also included in Fig.3. It appears that the latter points follow quite closely the power law approximation.

As for the limit pressure p_{limit}, it was determined by putting $\gamma = 1$ into Eq.21 and the results are also reported in Table 3. Examination of the various entries shows that it varies in a very small range, from 1608.3 kPa to 1609.6 kPa. Further, comparison between Eqs.21 and 12 shows that for the limit pressure to be unique, the rigidity index obtained from hyperbolic model should be approximately equal to twice the value determined on the basis of the inverse hyperbolic approach. This is perfectly borne out by the results presented in Table 1 and 3.

3.4 Linear Elastic Perfectly Plastic Response

Finally, in order to examine the possibility that a simple linearly elastic perfectly plastic (Tresca) stress-strain relationship of the form:

$$\tau = G\gamma\,, \qquad \gamma \leq \gamma_y = S_u / G \qquad [24a]$$

and

$$\tau = S_u\,, \qquad \gamma > \gamma_y = S_u / G \qquad [24b]$$

might be appropriate for the clay, these equations were substituted in Eq.2 to obtain the well-known pressure-expansion relationships (Gibson and Anderson, 1961):

$$p = p_0 + G\gamma\,, \qquad \gamma \leq \gamma_y = S_u / G \qquad [25a]$$

and

$$p = p_0 + S_u\left(1 + \ln\frac{\gamma}{\gamma_y}\right), \qquad \gamma > \gamma_y \qquad [25b]$$

Again, the limit pressure may be found by putting $\gamma = 1$ into Eq.25b.

Instead of performing two separate regression analyses, that is, one for elastic phase of deformation and the other for the plastic response, it was deemed preferable to obtain by iteration a good fit to the experimental pressure-expansion curve. This was done by adjusting the values of the parameters p_0 and G_{max}.

Two such solutions are reported in Table 4 and are compared in Fig.4 with the experimental pressure-expansion curve. Examination of the data shown in this figure indicates that the solution which corresponds to p_0 = 496 kPa, S_u = 178 kPa, G_{max} = 34563 kPa, and γ_y = 0.00515, compares well with the experimental results. In addition, the limit pressure p_{limit} which was calculated on the basis of Eq.25b for $\gamma = 1$ varies between 1610.1 kPa and 1611.8 kPa.

A stress-strain curve based upon the solution just mentioned is also shown in Fig.3. Examination of the various relationships reported in this figures indicates that although the simple linearly elastic perfectly plastic solution is much softer than the previously obtained relationships, it nevertheless gives a good fit to the experimental pressure-expansion curve of Fig.4.

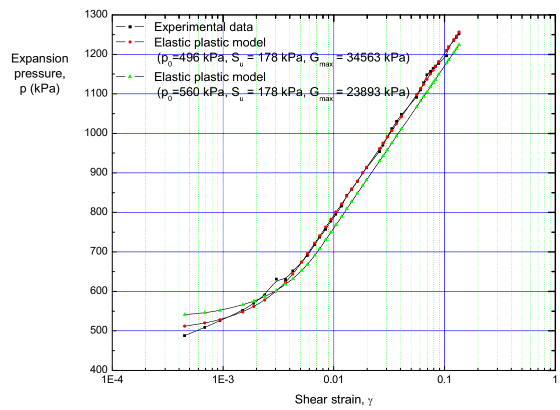

Figure.4: Comparison of experimental data with linearly elastic perfectly plastic responses.

4. DISCUSSION

It appears at first sight that the inverse hyperbolic sine solution obtained in this study and that of Bolton and Whittle (1999) are quite similar. Indeed, linear regression analyses yielded almost identical values for the coefficient of correlation.

There is, however, a sight divergence that arises between the two approaches. While the value of G_{max} is finite in the present approach as found from Eq.7, that determined by using the power law representation is infinite. Indeed, differentiation of Eq.17a gives:

$$G = \frac{d\tau}{d\gamma} = \eta \beta^2 \gamma^{\beta - 1} \quad [26]$$

which, when evaluated at $\gamma = 0$, leads to $G_{max} = \infty$, since $\beta < 1$. Such a particular behaviour of the power law representation at the origin is thought to be inappropriate for clay.

As for the simple hyperbolic stress-strain curve, it is shown that it is much stiffer than the inverse hyperbolic sine law. In addition, it is indicated that although the linearly elastic perfectly plastic criterion fits reasonably well the experimental pressure-expansion relationship, it nevertheless fails to represent the non-linear stress-strain response of the material at small strains.

As a final point worth of discussion, it appears from the results shown in Fig.2 and 3, that while any of the curve-fitted relationships is more or less adequate to represent the experimental pressure-expansion date, the derived stress-strain curves are however all quite different. This represents a formidable task for the geotechnical engineer because the derived stress-strain curve is dependent upon an assumed relationship for the pressure-expansion curve. It is thus impossible to make an objective assumption, even if one makes use of statistical methods. The difficulty is linked to the fact that the stress-strain curve is obtained from the differentiation of the pressure-expansion relationship. However, the reverse problem, that is, the task of obtaining the pressure-expansion curve from a known stress-strain relationship, is much simpler, because of the integration procedure.

5. CONCLUSIONS

This technical paper presents a method to obtain the stress-strain curve of clay from undrained plane-strain pressuremeter tests. The experimental radial pressure versus shear strain curve is approximated by an inverse hyperbolic sine function. The resulting stress-strain curve can be described as a non-linear workhardening soil model, having a finite modulus at the origin.

Because the stress-strain curve was obtained using Palmer's approach, it was not necessary to separate the soil response into elastic and plastic components. Compared to the stress-strain curve based upon a power law representation, that obtained in this study was stiffer.

It was also found that a simple hyperbolic stress-strain curve resulted in a much stiffer response compared to both the inverse hyperbolic sine law and the power law representations. As for the simple linearly elastic perfectly plastic (Tresca) response, it failed to capture the pronounced non-linear stress-strain behaviour at small strains.

6. ACKNOWLEDGMENTS

The authors express their gratitude to the National Research Council of Canada for the financial support received in this study.

7. REFERENCES

Bolton, M.D., and Whittle, R.W. 1999. A non-linear elastic/perfectly plastic analysis for plane strain undrained expansion tests. Géotechnique 49(1): 133-141.

Gibson, R.E., and Anderson, W.F. 1961. In situ measurement of soil properties with the pressuremeter. Civil Engineering and Public Works Review, 56: 615-618.

Hill, R. 1950. The mathematical theory of plasticity. Oxford University Press, London.

Ladanyi, B. 1972. In situ determination of undrained stress-strain behaviour of sensitive clays with the pressuremeter. Canadian Geotechnical Journal, 9(3): 313-319.

Ladanyi, B. 1975. Bearing capacity of strip footings in frozen soils. Canadian Geotechnical Journal, 12(3): 393-407.

Ladanyi, B., and Johnson, G.H. 1974. Behaviour of circular footings and plate anchors embedded in permafrost. Canadian Geotechnical Journal, 11(3): 531-552.

Mitchell, J.K. 1993. Fundamentals of Soils Behaviour. 2nd Edition, John Wiley & Sons, Inc., New York.

Palmer, A.C. 1972. Undrained plane-strain expansion of a cylindrical cavity in clay: a simple interpretation of the pressuremeter test. Géotechnique 22(3): 451-457.

Silvestri, V., Yong, R.N., Soulié, M., and Gabriel, F. 1986. Controlled-strain, controlled-gradient, and standard consolidation testing of sensitive clays. Proceedings, Symposium on Consolidation of Soils: Testing and Evaluation; Fort Lauderdale, Fla; ASTM STP 892, R.N. Yong and F.C. Townsend, Eds.; American Society for Testing and Materials, Philadelphia, pp. 433-450.

8. APPENDIX A

Table 1: Results of regression analyses on inverse hyperbolic sine law.

p_0 (kPa)	Regression analyses			p_{limit} (kPa)
	$\hat{a}$	$\hat{b} = G_{max} / S_u$	Coefficient. of correlation, r	
450	0.05825	338.3	0.99908	1610.1
460	0.02958	320.3	0.99916	1610.3
470	0.0170	302.7	0.99908	1610.3
440*	0	360.5	0.99776	1611.4
450*	0	340.8	0.99777	1611.4
460*	0	322.4	0.99772	1611.5
470*	0	304.6	0.99760	1611.4

*Regression line forced to pass through the origin.

Table 2: Results of regression analyses on power law approximation.

P_0 (kPa)	Regression analyses				γ_y	P_{limit} (kPa
	$\hat{a}$=lnη	η (kPa)	$\hat{b} = \beta$	Coefficient of correlation, r		
410	8.24274	3800	0.50376	0.99960	0.00896	1602.6
420	8.36831	4308	0.53536	0.99969	0.00836	1604.1
430	8.52085	5018	0.57240	0.99947	0.00776	1605.8
440	8.71371	6086	0.61728	0.99879	0.00714	1608.0
450	8.95206	7724	0.67142	0.99727	0.00659	1609.1
460	9.26656	10578	0.74053	0.99411	0.00603	1610.1

Table 3: Results of regression analyses on simple hyperbolic law approximation

p_0 (kPa)	$\hat{a}$	$\hat{b} = G_{max} / S_u$	Coefficient. of correlation, r	p_{limit} (kPa)
440	-0.5546	713.3	0.99902	1609.6
450	-0.5782	673.1	0.99905	1609.2
460	-0.6196	637.5	0.99905	1609.3
470	-0.6270	601.6	0.99899	1609.3
440*	0	709.0	0.99775	1608.3
450*	0	669.5	0.99793	1608.4
460*	0	633.2	0.99784	1608.5

*Regression line forced to pass trough the origin

Table 4: Results of linearly elastic perfectly plastic response approximation

p_0 (kPa)	S_u (kPa)	G_{max}/S_u	γ_y	p_{limit} (kPa)
496	178	34563	194	1611.8
560	178	23893	134	1610.1